

# An integrated methodology to assess future water resources under land use and climate change: an application to the Tahadart drainage basin (Morocco)

M. Antonellini · T. Dentinho · A. Khattabi ·  
E. Masson · P. N. Mollema · V. Silva · P. Silveira

Received: 4 February 2013 / Accepted: 27 May 2013  
© Springer-Verlag Berlin Heidelberg 2013

**Abstract** The assessment of freshwater resources in a drainage basin is not only dependent on its hydrologic parameters but also on the socio-economic system driving development in the watershed area; the socio-economic aspect, that is often neglected in hydrologic studies, is one of the novelties of this study. The aim of this paper is twofold: (1) presenting an integrated working methodology and (2) studying a local case of a North African watershed where scarce field data are available. Using this integrated methodology, the effects of climate and land use change on the water resources and the economic development of the Tahadart drainage basin in Northern Morocco have been evaluated. Water salinization, tourism, urbanization, and water withdrawals are a threat to water resources that will increase with future climate change. The Tahadart Basin (Morocco 1,145 km<sup>2</sup>) is characterized by rain-fed agriculture and by the presence of two water retention basins. Assessment of the effects of climate and land use change on this drainage basin was based on current and future land cover maps obtained from spatial interactions models, climate data (current and future; scenario A1b for the period 2080–2100), and hydrological models for water budget calculations. Land use suitability maps were

designed assuming a A1b Special Report on Emissions Scenarios socio-economic development scenario. The most important conclusions for the period 2080–2100 are the following: (1) Freshwater availability within the watershed will likely be affected by a strong increase in evaporation from open water surface bodies due to increased temperature. This increase in evaporation will limit the amount of freshwater that can be stored in the surface reservoirs. (2) Sea level rise will cause flooding and salinization of the coastal area. (3) The risk for drought in winter is likely to increase. The methodology used in this paper is integrated into a decision support tool that is used to quantify change in land use and water resources.

**Keywords** Freshwater resources management · Salt water intrusion vulnerability · Land use planning · Coastal drainage basins · Decision support tool · Climate change

## Introduction

Water resources management is an important issue for the Integrated Coastal Zone Management Protocol (European Union Commission 2009, 2010) both in the European and Mediterranean regions. Freshwater resources, including ground water, have specific vulnerability issues in a coastal area. Coastal zones are among the most densely populated in the world (Small and Nicholls 2003) putting an enormous pressure on water demand. The edge of the sea with its natural and human-induced fluctuations (erosion, climate change, urbanization) maintains the coastal territory and its resources in a state of continuous change and transition (Vallega 1999; European Union Commission 2009). Therefore, the sustainable use of freshwater in agreement with land cover is an important issue in coastal drainage

M. Antonellini (✉) · P. N. Mollema  
IGRG, University of Bologna, Bologna, Italy  
e-mail: m.antonellini@unibo.it

T. Dentinho · V. Silva · P. Silveira  
Universidade dos Açores, Terceira, Portugal

A. Khattabi  
Ecole Nationale Forestière d'Ingenieures, Rabat, Morocco

E. Masson  
Université des Sciences et Technologies, Lille, France

basins (European Union Commission 2009; Schanze et al. 2012). Another important issue is avoiding ground water salinization (Custodio 2010; Carneiro et al. 2010).

In the future, the availability of freshwater resources in the coastal zones will be challenged by the trends of climate change that predict higher temperatures and lower rainfall in many Mediterranean basins (Giupponi and Mordechai 2003) combined with a general increase of sea level (Solomon et al. 2007). Given that climate change requires long-term planning to adapt to the future conditions, administrators are faced with the issue of selecting appropriate policies to steer a sustainable land use development for future freshwater needs and availability.

The main objective of this work has been to develop a methodology to evaluate the effects of climate and land use change on the water budget of drainage basins that include not only the hydrologic parameters but also the characteristics of the socio-economic environment driving the development of a coastal area. The methodology is demonstrated on a local case study in the Tahadart Basin (Northern Morocco) where tourism, urbanization, salinization, demands of water for the city of Tangiers and for energy production are already generating a strong pressure on the resource. The basin problems are similar to those of other watersheds in North Africa (Revenga et al. 1998; Carneiro et al. 2010; Fernandes et al. 2010; Trabelsi et al. 2012). The data available for the basin considered are relatively scarce, which is a common condition for many watersheds in developing countries; the methodology that will be presented proposes the use of relatively cheap technologies, such as remote sensing (Batelaan and De Smedt 2007), to acquire some of the data needed for the study.

The effect of seasonal variations in the water budget of Mediterranean coastal watersheds and the consequences of this seasonality on ground water quality in the coastal aquifers are important issues (Mollema et al. 2012; Mollema and Antonellini 2013) and are considered in this study by evaluating the water budgets not only at yearly but also at seasonal periods. This is even more crucial since climate change may enhance the drought in the dry periods and the precipitation in the wet periods (IPCC 2007).

The methodology that has been developed for this study includes analysis of today land use and climate data, future climate models temperature and rainfall data (A1b SRES; IPCC 2007), and spatial interaction models (Dentinho and Silveira 2010). The complexity of data handling among different models was integrated into a simple scenario evaluation and decision support tool (WATER\_DST) in an effort similar to that described by Kalbacher et al. (2012) for the IWAS-Toolbox.

The workflow developed in this research project may be used by local stakeholders or authorities with limited economic resources to take more informed decisions in the

area of land use and water management in view of climate change.

### Drainage basins characteristics

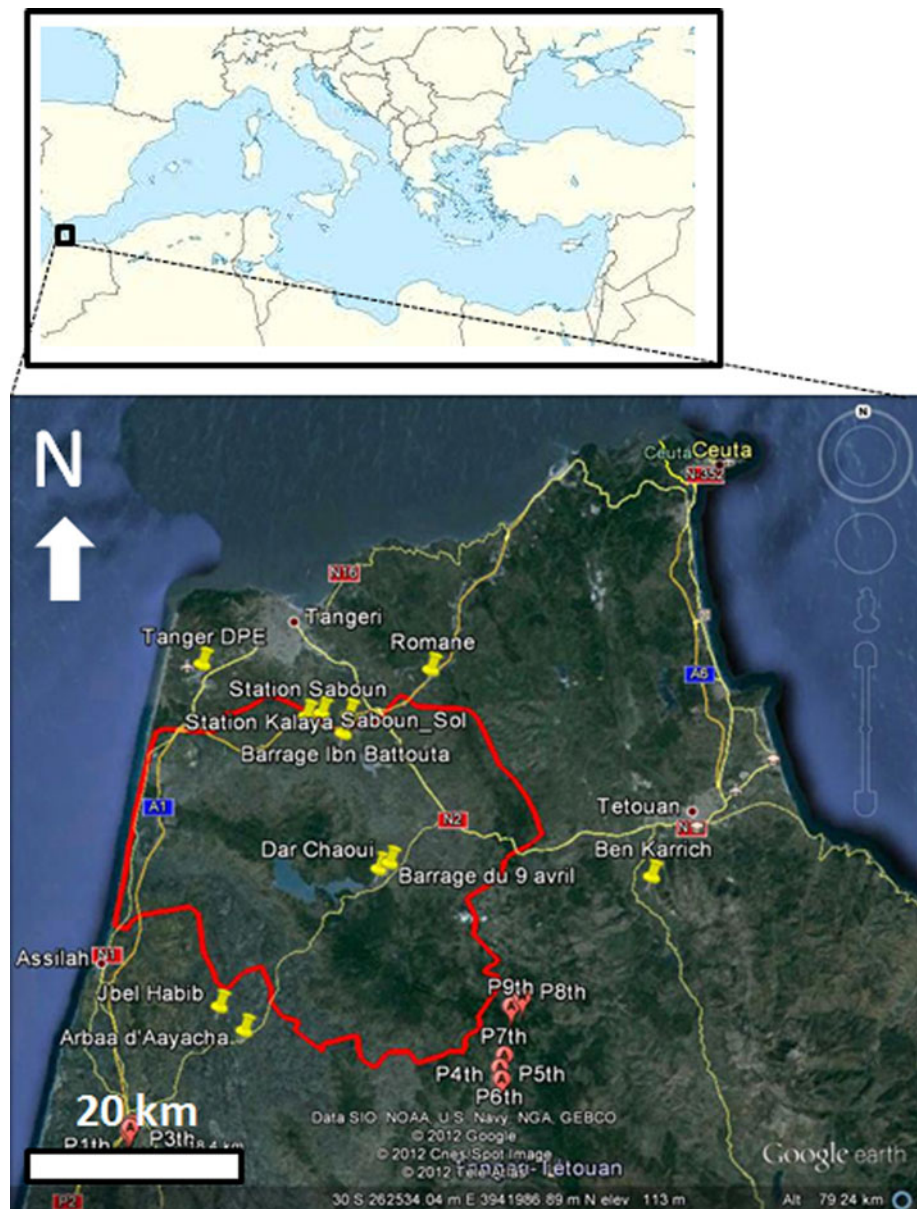
The Tahadart basin (Fig. 1) is located between LAT. 35°21'24"N and LAT. 35°42'09"N and LONG. 6°1'15"W and LONG. 5°32'00"W. The surface area of the watershed is 1,190 km<sup>2</sup>. The geomorphology of the basin is characterized by an alluvial plain in the west, central hills and mountainous areas in the southeast and in the east. Two major artificial water reservoirs are located within the Tahadart watershed: the “Hachef” or “5 April” (270 million m<sup>3</sup>) and the “Ibn Batouta” (44 million m<sup>3</sup>) reservoirs provide the drinking water supply for the city of Tangiers. The Tahadart basin has a Mediterranean climate with a winter (or “wet period” when most of the rainfall occurs) from September through February and a summer (or “dry period” when almost no rainfall occurs) from March through August. Land use (Fig. 2) consists mainly of rain-fed agriculture and native vegetation consisting of trees and shrubs. The critical issues in the basin are essentially three: (1) the extensive coastal urbanization driven by tourism development is causing a destruction of the dunes and salinization of the ground water; (2) changes in rainfall patterns that may affect the local rain-fed agriculture and the drinking water availability in the surface reservoirs supplying Tangiers; (3) the high soil erosion rates and the amount of sediments filling into the surface water reservoirs that cause a decrease in capacity ranging from 0.25 to 1.6 % per year (Fox et al. 1997).

### Methods

The workflow methodology presented in this paper is summarized in Fig. 3. The starting point was a map of land use and a series of climate data including monthly temperatures (min, max and average), rainfall, relative humidity (min, max and average), wind speed, and cloud coverage (or in alternative monthly daily sun hours). The following step was to obtain the future climate data for the IPCC scenarios (IPCC 2007) chosen. In this paper, we consider the “moderate” scenario A1b for the Tahadart basin. This scenario envisions a globalized world characterized by rapid economic growth, a global population that reaches 9 billion in 2050 and then gradually declines a quick spread of new and efficient technologies and a mix of non-renewable and renewable energy sources (IPCC 2007).

Future (2080–2100) land use maps for scenario A1b are constructed using economic models such as the spatial interaction models (Silveira et al. 2009) detailed in the next

**Fig. 1** Index map containing the outline (red line) of the Tahadart Basin in North Morocco with its location in the Mediterranean area. The yellow pins represent the location of the meteorological stations used in this study



sections. The evaluation of the effects of land use and climate change on the hydrological budget is performed by data elaboration and mapping within WATER\_DST (Fig. 3). The annual difference between rainfall and actual evapotranspiration as well as the seasonal differences in the “dry” and “wet” periods has been considered. In the following, we explain the different steps of the methodology and the models used.

#### Land use maps

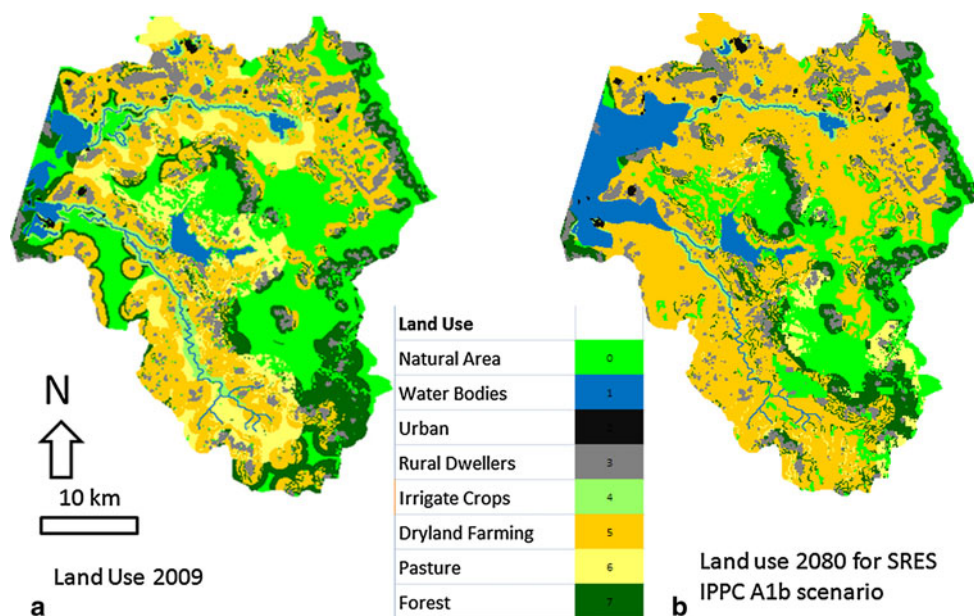
Different land uses have different water needs and have a different impact on the hydrological cycle (Batelaan and De Smedt 2007). For this reason, preliminary to any scenario analysis was to create the current land use map

(Fig. 2a). Since no land use map was available, a map was created using SPOT 5 satellite images with ground control (Gao and Skillkorn 1998). The SPOT 5 multi-temporal datasets used are (a) one archive dataset (June 2008) in drought year conditions (below average rainfall), (b) three acquisitions programming datasets (April 2009; July 2009 and September 2009) in wet year conditions (above average rainfall), (c) 16 bands multi-temporal datasets for surface water monitoring, and (d) Native 10 m XS sensor data.

Field training and validation of the land use map were conducted in June 2009. With a GPS, 312 points were acquired both for landscape and land use samples with 400 photos and field comments. This field material was used to validate an object based image analysis (OBIA) and build a



**Fig. 2** Land use maps for the Tahadart basin. **a** Land use for the Tahadart basin obtained from SPOT 5 image analysis and field surveys at the year 2009. **b** Land use at the year 2080 under A1b SRES scenario conditions checked with the land suitability maps for the same period obtained from the spatial interaction models



land cover map for the year 2009 (image acquisition period) with 8 classes (Table 1) as defined by the project CORINE LAND COVER (2011): agriculture (rain-fed), natural areas (mosaic vegetation), urban areas, open water, and wetlands. The OBIA methodology allows to extract information (i.e. land use) from remotely sensed images by partitioning the imagery into meaningful real-world image-objects, and assessing their characteristics through spatial, spectral and temporal scale. The technical steps required by a OBIA analysis include image segmentation, pixel attribution, classification and the ability to query and link individual objects (also known as segments) in space and time (Blaschke 2010). GIS maps databases were created to compare and overlay different geomorphologic, geological, and land attributes.

#### Climate data

The scope of this study was to show a methodology in which the predictions of climate models may be integrated into a workflow to evaluate their effects on land use and the hydrologic budget. The future climate scenario that has been considered is the SRES A1b (IPCC 2007) for the 2080–2100 period. This emission scenario (SRES A1b) has been chosen, because of its intermediate character in socioeconomic development, whereas the far-in-the-future timeframe (2080–2100) has been adopted to better distinguish the future conditions from the actual ones. The land use modeling performed has a reference state that is the “current land use” while the data used in climate models usually consider a historical period as a “reference state” (1960–1990).

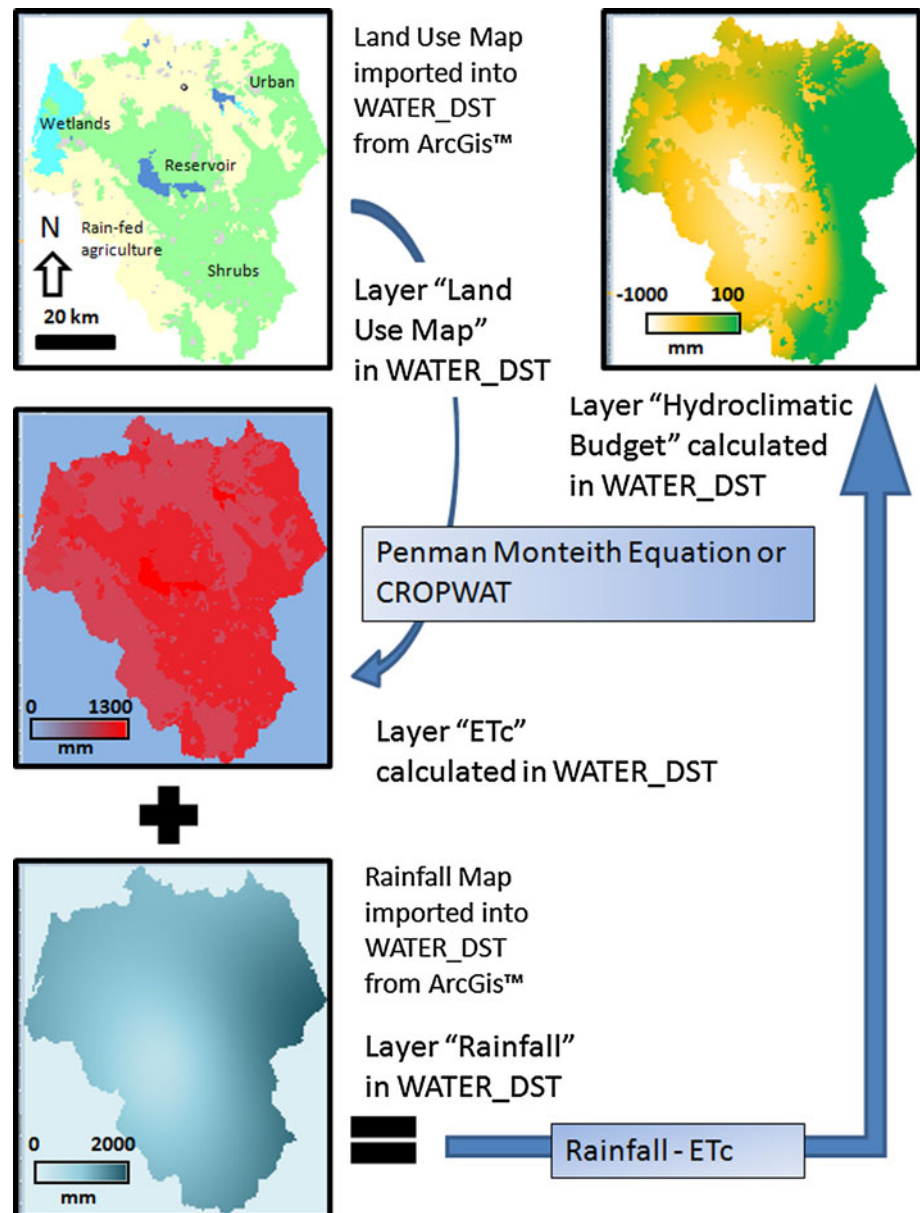
The source of the current climate data (1940–2009 period) for the Tahadart basin is from 10 meteorological stations (Moroccan Government): 10 for rainfall, 3 for temperature, and 3 for wind velocity data. The data have been processed as follows: monthly average values of temperature and precipitation were calculated and then averaged again over two periods 1960–1990 and 1977–2009. Monthly data have then been grouped in seasons. The average annual precipitation and temperature in the basin are 730 mm and 17.5 °C, respectively.

The Regional Climate Models (RCMs) of the PRUDENCE project (2011) cover Europe and some of the North Africa coastal area including the Tahadart basin. In particular, the DMI 25 km (Danish Meteorological Institute) resolution grid data from the PRUDENCE (2011) project for the Tahadart basin show a change in climate parameters not only with respect to the reference conditions (1960–1990) but also with the average climate of the last decade. For this reason, the RCMs climate data for the Tahadart basin from the PRUDENCE project (2011) have been used. The future climate data for the Tahadart basin were taken directly from the DMI maps at seasonal intervals published in the PRUDENCE project report (2011). The future scenario was chosen to be the A1b for the years 2080–2100.

#### Hydrological water budgets

The hydrological budget of a basin is the basis for the calculation of the water resources in a given watershed. A simple expression of the yearly water budget equation (Fetter 2001; Healy 2011; Mollema et al. 2012) is the following:

**Fig. 3** Structure of the WATER\_DST application: land cover layer, crop evapotranspiration layer computed from the Penman–Monteith equation or from CROPWAT, rainfall layer, and output layer representing the hydroclimatic budget



$$P = R + ET + I \pm \Delta W \quad (1)$$

where  $P$  is the rainfall in mm/year,  $R$  is the runoff in mm/year,  $ET$  is the evapotranspiration in mm/year,  $I$  is the infiltration in mm/year,  $\Delta W$  is the import/export in and out of the basin in mm/year.

This is the basic formula that is implemented in the data elaboration workflow (within WATER\_DST or the GIS). The parameters above are either assigned by the user ( $P$ ,  $\Delta W$ ,  $R$ ) or computed ( $ET$ ,  $I$ ) by spreadsheets added to the tool (WATER\_DST). The rainfall is calculated from pluviometers located in stations within the drainage basin whereas  $\Delta W$  and  $R$  have to be obtained by independent means (Maidment 1992) or, if present, by the watershed authorities that track river flow and manage water import and export.

Runoff ( $R$ ), Infiltration ( $I$ ), and Evapotranspiration ( $ET$ ) are all influenced by different land uses. Infiltration is a difficult parameter to quantify (Healy 2011); potential infiltration, however, can be estimated by the following relationships if we assume negligible the other contributions to the budget

$$I = P - R - ET \quad (2)$$

The evapotranspiration can be assigned for every agricultural land use (Mollema et al. 2012) using for example CROPWAT (Smith et al. 1992), which is based on the Penman–Monteith equation (Penman 1948; Monteith 1973). It can also be calculated within WATER\_DST or in a GIS software. In both cases, the parameters needed to compute the Penman–Monteith equation and the crop coefficients ( $K_c$ ) must be provided by the user.

**Table 1** Land use following CORINE classification and methodology for computing actual evapotranspiration in the different land use plots

CORINE land use class	Evaporation/evapotranspiration calculation method
Forestry production area	CROPWAT or Penman eq w/Kc
Horticulture and fruit area	CROPWAT or Penman eq w/Kc
Agricultural area (irrigated or rain-fed)	CROPWAT or Penman eq w/Kc
Mineral extraction sites	Penman Eq. open water
Natural area	CROPWAT or Penman eq w/Kc
Urban area	Evaporation = Rainfall = Drainage
Water areas	Penman Eq. open water
Wetlands	CROPWAT or Penman eq w/Kc

Evaporation from open surface water depends on many different climate variables: wind, air humidity, air temperature, vapor pressure deficit, etc. The open water potential evaporation ( $E_p$ ) is calculated with the recommended equation by Maidment (1992, p. 4–14), which is based on the Penman–Monteith equation that describes how the available energy from the sun is used for evapotranspiration of water, taking into account all types of resistances provided by vegetation in case of evapotranspiration.

The FAO Penman–Monteith method was implemented in CROPWAT to estimate the reference crop evapotranspiration  $ET_o$  (Smith et al. 1992; CROPWAT 2011). The reference evapotranspiration  $ET_o$  is a standard used to compare evapotranspiration of crops or bare soil at different periods of the year or in different regions and it is only dependent on climate parameters. The crop evapotranspiration under standard conditions, denoted as  $ET_c$ , is the evapotranspiration from disease-free, well-fertilized crops, grown in large fields, under optimum soil water conditions, and achieving full production under the given climate conditions and is obtained by the following equation:

$$ET_c = K_c \times ET_o \quad (3)$$

where  $K_c$  is the crop coefficient that is determined experimentally (Smith et al. 1992).

The program CROPWAT calculates a monthly water budget using average climate values. The soil moisture deficit and amount of water needed for irrigation depend not only on the climate, but also on the type of soil. The soil moisture needed for CROPWAT calculations is estimated using the Soil Water Characteristics Hydraulic properties calculator by Saxton (2003).

Within WATER\_DST, it is possible to compute the change in crop type or land use on freshwater budget; this is done by defining the “hydroclimatic budget” as

$$\text{Hydroclimatic budget} = P - ET_c \quad (4)$$

The hydroclimatic budget can be negative or positive.

The lack of detailed hydrometric gage measurements in the Tahadart basin does not allow for a precise quantification of the runoff. It was, however, possible to compute the change in unit runoff caused by the change in land use (Table 2). This was done using average runoff coefficients associated with different land uses (Maidment 1992) as input for the rationale method (Maidment 1992); in this way, the change in land use from 2009 to 2080 provides a way to estimate the change in unit runoff intensity.

#### Salt-water intrusion indicator

Sea level rise and climate change effects on the hydrologic cycle, such as a change in aquifer recharge, may affect salinization of the surface water and of the ground water in the coastal zone of a watershed (Werner and Simmons 2009). A first approach to the problem is to quantify how much surface of the coastal zone is invaded by salt-water as a result of sea level rise and this can be easily done using an elevation DEM coupled with maps of land use change. A second approach considers both the sea level rise and the change in potential recharge between the year 2009 and

**Table 2** Change in land use and in unit runoff for the Tahadart basin

Land use (ha)	2009	2080	C value	2009—Unit Runoff (m <sup>3</sup> /sec) <sup>a</sup>	2080—Unit Runoff (m <sup>3</sup> /sec) <sup>a</sup>
Natural area	28,146	19,736	0.1	7.9	5.5
Water bodies	5,034	9,800	0	0.0	0.0
Urban	560	637	0.7	1.1	1.2
Rural dwellers	11,164	11,622	0.4	12.5	13.0
Irrigate crops	4,268	1,711	0.3	3.6	1.4
Dryland farming	34,284	52,652	0.3	28.8	44.2
Pasture	13,283	3,531	0.2	7.4	2.0
Forest	15,584	12,634	0.1	4.4	3.5
Total	112,323	112,323		65.7	71.0

<sup>a</sup> Unit Runoff (per unit rainfall intensity mm/hr)—m<sup>3</sup>/sec

2080 and its effect on the sea water intrusion vulnerability. In this paper, salinization of the ground water in the unconfined aquifer of the Tahadart Basin coastal zone has been characterized using the vulnerability indicator  $M$  presented by Werner et al. (2012). The indicator  $M$  is a mixed convection ratio defined as:

$$M = \frac{K\delta(1 + \delta)z_0^2}{W_{\text{net}}x_n^2}, \quad (5)$$

where  $K$  (m/day) is the hydraulic conductivity of the aquifer,  $z_0$  (m) is the thickness of the unconfined aquifer,  $W_{\text{net}}$  (m<sup>2</sup>/year) is the recharge of the unconfined aquifer,  $x_n$  is the inland distance of the no flow boundary, and  $\delta$  is a dimensionless density term defined as

$$\delta = \frac{(\rho_s - \rho_f)}{\rho_f} \quad (6)$$

where  $\rho_s$  (Kg/m<sup>3</sup>) is the density of sea-water and  $\rho_f$  (Kg/m<sup>3</sup>) is the density of freshwater. The numerator of  $M$  reflects density-driven processes acting to extend the freshwater-salt water interface landward, whereas the denominator of  $M$  accounts for freshwater advection that opposes the inland migration of the salt water wedge (Werner et al. 2012). The  $M$  values varies from 0 to 1; low  $M$  values stand for aquifers with low vulnerability to salinization, high  $M$  values are for aquifers vulnerable to salinization.

The  $M$  indicator has been modified in this study to accommodate for changes in recharge and sea level rise due to climate change by introducing the  $\alpha$  ratio between the net recharge of the aquifer at the year 2080 ( $W_{\text{net}2080}$ ) and the net recharge of the aquifer at the year 2009 ( $W_{\text{net}2009}$ ). Potential recharge can be inferred from the surplus in hydroclimatic budget for the wet (winter) period in 2009 and 2080. We assume that this winter period surplus spread over the entire period of the year represents the effective recharge of the ground water. This recharge allows for a flux to the sea that contrasts salt water intrusion in the ground water. The increase in sea level due to climate change  $\Delta z$  (m) can be implemented by increasing the thickness of the aquifer at the coastline as suggested by Werner and Simmons (2009). To do this, in this study, the parameter  $\beta$  was defined as:

$$\beta = \left(1 + \frac{\Delta z}{z_0}\right) \quad (7)$$

so that the  $M$  parameter can be re-written to accommodate the effects of a change in sea level and in recharge driven by climate change ( $M_{\text{cc}}$ ):

$$M_{\text{cc}} = \frac{K\delta(1 + \delta)\beta^2 z_0^2}{\alpha W_{\text{net}}x_n^2} \quad (8)$$

It is reasonable to assume that parameters such as  $K$ ,  $\delta$ , and  $x_n$  do not vary much as a result of climate change, so that  $M_{\text{cc}}$  can be re-written as:

$$M_{\text{cc}} = \frac{\beta^2}{\alpha} M \quad (9)$$

In this way, the effects of climate change in the coastal zone of the Tahadart Basin can be evaluated, in a relative way.

### Spatial interaction models

The determination of the future land use is an important issue that needs to be resolved when evaluating hydrologic budgets under future climate scenarios. The evaluation of local changes due to climate change is analyzed in most studies without considering the local socio-economic variables, like commuting patterns, agricultural productivity, and other anthropogenic variables that model human behavior at local level. Furthermore, it is very simplistic to consider land use in the future the same as the current one or evolved according to rules that extrapolate to the future the current trends in land use or climate change (this may be considered similar to a Business As Usual—BAU scenario). This issue was addressed using a Spatial Interaction Model (Silveira et al. 2009; Dentinho and Silveira 2010) with land use for the simulation of different scenarios of possible changes in the Tahadart basin. Environmental data including total annual precipitation, average annual temperature, soil classification, geomorphologic information, for current and future climate, coupled with human information, such as population, employment information, agricultural information (production, productivity, consumption), mobility patterns, were used to implement the model for this region.

Current land use information was used to calibrate the spatial interaction model for the current scenario. The IPCC (2007) scenario on climate change (environmental variables), A1B, was used, in conjunction with the SRES economic predictions, for the modeling of the Land Use scenario for 2080.

The spatial interaction multicriteria model determines how suitable the soil is under current and future climate scenarios for a certain use, taking into account soil type, climate, and economic aspects such as the distribution of residential, industrial, agricultural, and employment facilities.

The model distributes the people residency (the place where people live) and their employment (the place where people work) to different zones of the region, taking into account the distances between those zones and their attractiveness. In the spatial interaction model of land use, it is assumed that residents and each type of employment



both generate land use patterns based on coefficients of land use for each activity (Silveira et al. 2009). The implementation of the model used in our research is similar to that presented by Dentinho and Silveira (2010). In this latter paper, each zone was divided into 14 soil classes, and conflicts between different activities for the same soil class were solved through the calibration of the respective bid-rents, which are closely associated with the estimated factors of attractiveness. The appeal for people to live in a different zone (residency) was a weighted attractiveness of the various soil classes for urban use of that zone. In this study, each soil class in each zone is considered a sub-zone, influencing the distance matrix such that the attractiveness for residential use can be calibrated jointly with the bid-rents of the various soil classes for other urban activities.

The definition of soil classes is crucial for creating a scenario. All potential soil classes (deriving from the combination of different levels of average temperature, three levels of annual accumulated precipitation, different classes of land slope and different types of soils) were transformed into 12 soil classes (Table 3). To achieve that outcome, instead of defining the classes from the environmental conditions by themselves, new soil classes were defined considering the environmental conditions specific to the different activities. Table 3 reports the possible land uses for each soil class, which is the important constrain to build any future scenario land use map. An example of the land suitability classes for today and the 2080–2100 periods is given for the Tahadart basin in Fig. 4a and b.

This approach that permits only certain land uses for a given soil class type in the climate scenario considered allows to create more realistic future land use maps.

**Table 3** Soil suitability classes for land uses

Class	Urban	Touristic	Horticulture	Arable farming	Pasture	Forest
0						
1	X	X	X	X	X	X
2				X	X	X
3	X	X	X		X	X
4					X	X
5	X	X	X	X		X
6			X	X		X
7	X	X		X		X
8				X		X
9	X	X	X			X
10						X
11	X	X				X
12	X	X				

## Data elaboration

The scenario evaluation for the Tahadart basin has been carried out using both ArcGis<sup>TM</sup> and the WATER\_DST tool (Fig. 3) in a way to integrate geographic and climate data from the GIS, the spatial interaction models, and the hydrological models.

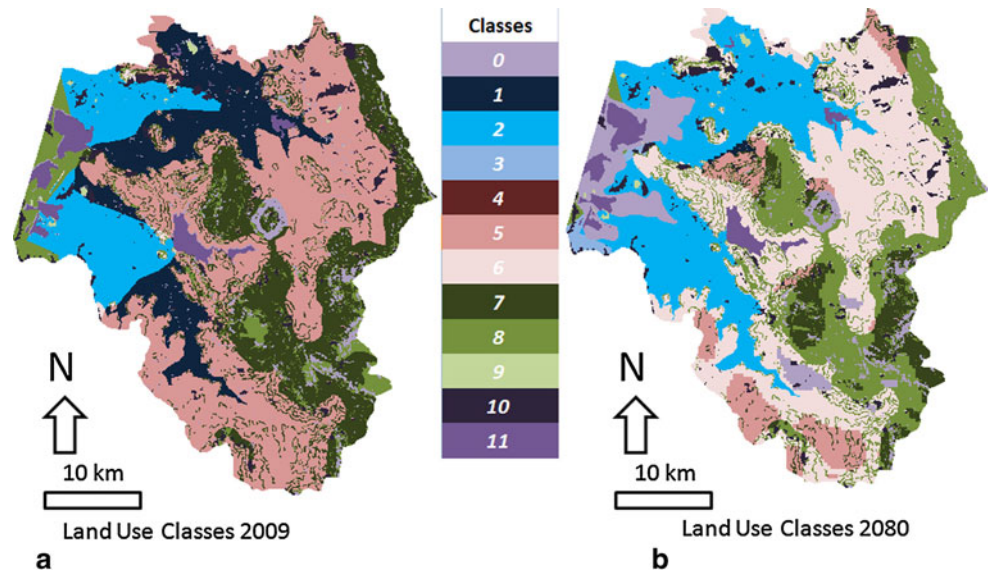
The decision support tool (WATER\_DST) has been developed in a mixed GIS (Geographic Information System)—spreadsheet environment (ArcGis<sup>TM</sup> for maps handling and Excel<sup>TM</sup> for calculation and data manipulation) in a way to integrate simple hydrological models, climate data (actual and future), and land use scenarios. The WATER\_DST results may be used as input for common multi-criteria decision analysis tools such as *mDSS* (Giupponi 2007). The user can decide to use different hydro-geological models rather than the water budget analysis embedded in the tool; this is simply accomplished by adding a layer/spreadsheet to WATER\_DST.

The maps obtained in ArcGis<sup>TM</sup> are gridded and then imported in Excel<sup>TM</sup>. Although the whole tool could have been developed in ArcGis<sup>TM</sup> by visual basics programming, it has been decided to use Excel<sup>TM</sup> for computations and data visualizations as many potential users are familiar with this software. In WATER\_DST, computations may be performed within a layer (spreadsheet) or among different layers. The land is divided into parcels (i.e. 100 × 100 m or 300 × 300 m grid) and to each parcel a cell (or the node of a grid) is assigned with a unique land use and/or a value for any other relevant attribute such as land elevation, soil type, etc. Different attribute values or information for any cell are stored in different spreadsheets within the WATER\_DST tool that correspond to “layers” in a GIS environment. WATER\_DST can quantify and visualize immediately the results of a scenario. Changing the land use value in a cell causes automatic recalculation of all output parameters in the corresponding cell within other spreadsheets or layers and so the effects of land use changes on freshwater resources in terms of total water budget are immediately visible. Conditional formatting of cells color is used to represent the data in map form directly within the spreadsheets. The basic layers needed for representing the water budget in a drainage basin and its future scenarios and the setup of WATER\_DST are represented in Fig. 3.

The data that need to be imported into the WATER\_DST tool are maps of land use suitability, actual land cover, soil type, digital elevation model (DEM) or topography, crop/vegetation type, rainfall, temperature, etc. If some of these data are not available in map form, or because the input data have been computed in separate software such as CROPWAT, they can be entered as single values in a table of the worksheet. Also some parameters,



**Fig. 4** Suitability classes for land use in the Tahadart basin for current conditions (a) and for those at the year 2080 (b). Land suitability has been computed from the spatial interaction models and the climate data from current stations and the climate models at the year 2080 (A1b SRES scenario). Explanations for the classes are given in Table 3



such as crop factors ( $K_c$ ) and indexes required for evapotranspiration calculation at different latitudes, need to be entered in a separate table.

The maps of the drainage basin (climate variables distribution, soil types distribution, digital elevation model, land use, etc.) may be used within or exported from ArcGis or any other software able to create a grid file from sparse data. The cells of the grid should have a side with a length adequate to the size of the basin and to the detail required by the analysis. In our example of the Tahadart basin, we have chosen a square cell with a side of 100 m (Fig. 2).

In order to calculate evaporation and evapotranspiration, WATER\_DST adopts the rules reported in Table 1 for the CORINE land cover. The spreadsheets/layers containing the different values of  $ET_c$  or evaporation from open water bodies are then added to calculate the total evapotranspiration spreadsheet (Fig. 3). The water budget or the hydroclimatic budget maps (Fig. 3) are obtained by subtracting the evapotranspiration grid from the grid with the rainfall data (or the data table entry). All data are then summarized in compact form within the output spreadsheet/layer (Fig. 3).

## Results

The land use map for the Tahadart Basin constructed from the satellite imagery with the OBIA methodology and the field checks is presented in Fig. 2a. The land use suitability classes for the year 2009 and the year 2080 obtained by applying the spatial interaction model statically are shown in Fig. 4a and b. The land use map at the year 2080 constructed from the land suitability classes and the impacts of sea level rise under SRES scenario A1b (0.5 m at the year 2080) on the current topography are shown in Fig. 2b. The

change (hectares) in land suitability classes (Table 3) is shown in compact form in Fig. 5a. The trend in classes change between 2009 and 2080 shows a strong decrease for classes 1, 5, and 7 matched by a strong increase in classes 0, 2, 6, and 8. The other classes have little change between 2009 and 2080 (Fig. 4a, b). The change (hectares) in land use is reported in compact form in Fig. 5b. It is apparent that the change in land use is less extensive than the change in classes (a single class, in fact, may be suitable for different land uses). Figure 2a, b shows the areal change in land use. The large increase in dry-land farming (Fig. 2a, b) by 2080 occurs at the expense of the irrigated crops, natural areas, and of the pastures. The increase in water bodies by 2080 occurs mostly in the coastal zone by a corresponding decrease in natural areas and forests.

The instantaneous runoff intensity per unit depth of rainfall (1 mm/h) changes from 65.7 m<sup>3</sup>/sec in 2009 to 71 m<sup>3</sup>/sec in 2080, an increase of almost 10 %.

Combining the maps of Fig. 2a and b, it was possible to construct the  $ET_c$  and hydroclimatic budget maps at the years 2009 and 2080 (Fig. 6). The same data are presented in compact form in Fig. 7a for the total area of the basin and in Fig. 7b by breaking down the contribution of the different land uses to  $ET_c$  and hydroclimatic budget. The summary data in Fig. 7a show that, in the Tahadart basin, the annual  $ET_c$  increases by about 200 mm from 2009 to 2080, with a more pronounced increase in the summer period (160 mm) with respect to the winter period (40 mm). The  $ET_c$  maps in Fig. 6a and b show that the evaporation/ $ET_c$  increases mostly in the coastal zone and where surface water bodies are present at the year 2080. The specific land use contributions to evaporation/ $ET_c$  reported in Fig. 7b show a strong increase in evaporation/ $ET_c$  from water bodies and from dry-land farming at the year 2080.

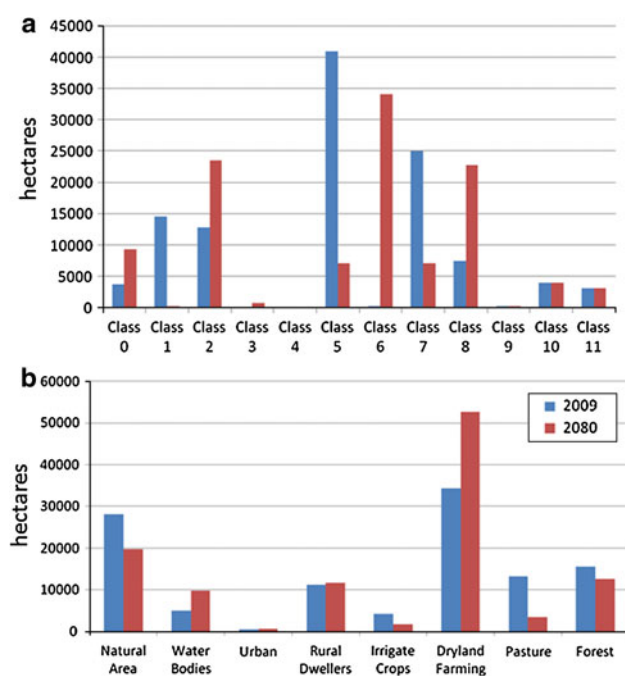


**Fig. 5** Change, expressed in hectares of land, for land suitability classes (a) and for land use (b) between 2009 conditions and 2080 A1b prediction. Explanations for the classes are given in Table 3

The aggregate data at basin level in Fig. 7a show an increase in the annual deficit from about  $-200$  mm in 2009 to  $-500$  mm in 2080, the winter period surplus decreases from  $380$  mm in 2009 to  $160$  mm in 2080, and the summer period deficit increases from  $-540$  to  $-640$  mm in 2080. The single land use contributions to the hydroclimatic budget (Fig. 7b) point out the increase to the deficit from the water bodies and from the dry-land farming. At basin level (Fig. 6c, d), the hydroclimatic deficit is larger, in both 2009 and 2080, within the coastal zone, the water reservoirs, and the urban areas. The maps in Fig. 8 quantify, at basin level, the increase in evaporation/ $ET_c$  (Figs. 8a–c) and in hydroclimatic budget deficit (Fig. 8d–f) between the year 2009 and the year 2080 in the annual, winter, and summer periods.

The results from the 2080 A1b land use scenario show the invasion of sea water into the lowlands of the Tahadart coastal zone and the increase in the area of water bodies from  $5,034$  hectares in 2009 to  $9,800$  hectares in 2080 for a sea level rise of  $0.5$  m (average expectations for the A1b scenario).

The computed  $W_{net2009}$  recharge at the year 2009 is  $346$  mm and the computed  $W_{net2080}$  recharge at the year 2080 is  $136$  mm, so that  $\alpha = 0.39$ . Table 4 reports the change in  $M_{cc}$  as a function of different unconfined aquifer thicknesses ( $z_0$ ), sea level rises and of the  $\alpha$  parameter computed for the A1b scenario. The largest relative increase in the  $M$  parameter ( $3.4$  factor) is for  $\Delta z = 1.5$  m,

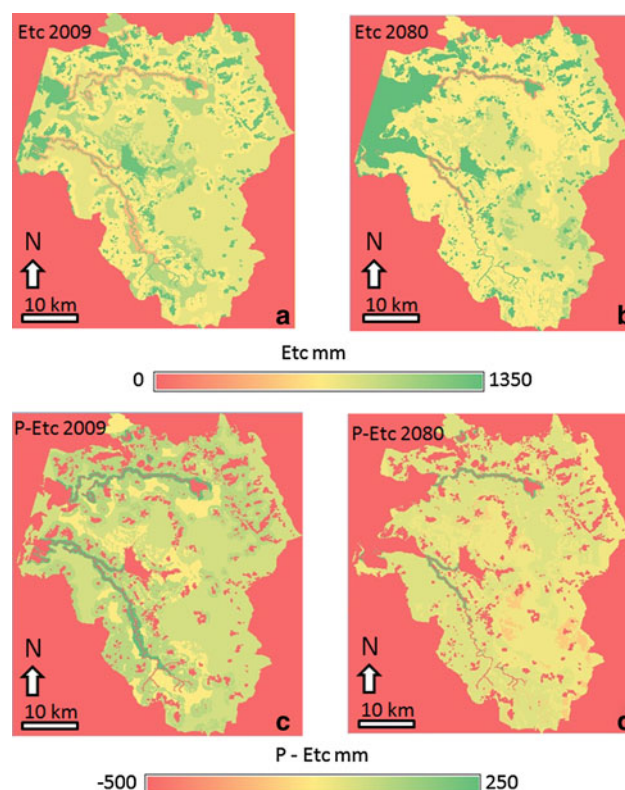


**Fig. 6**  $ET_c$  and Hydroclimatic maps of the Tahadart basin obtained from WATER\_DST: a annual  $ET_c$  in 2009, b annual  $ET_c$  in 2080 in the IPCC (2007) SRES A1b scenario, c annual hydroclimatic deficit (Rainfall- $ET_c$ ) at present time, d annual hydroclimatic deficit in 2080 in the IPCC (2007) SRES A1b scenario

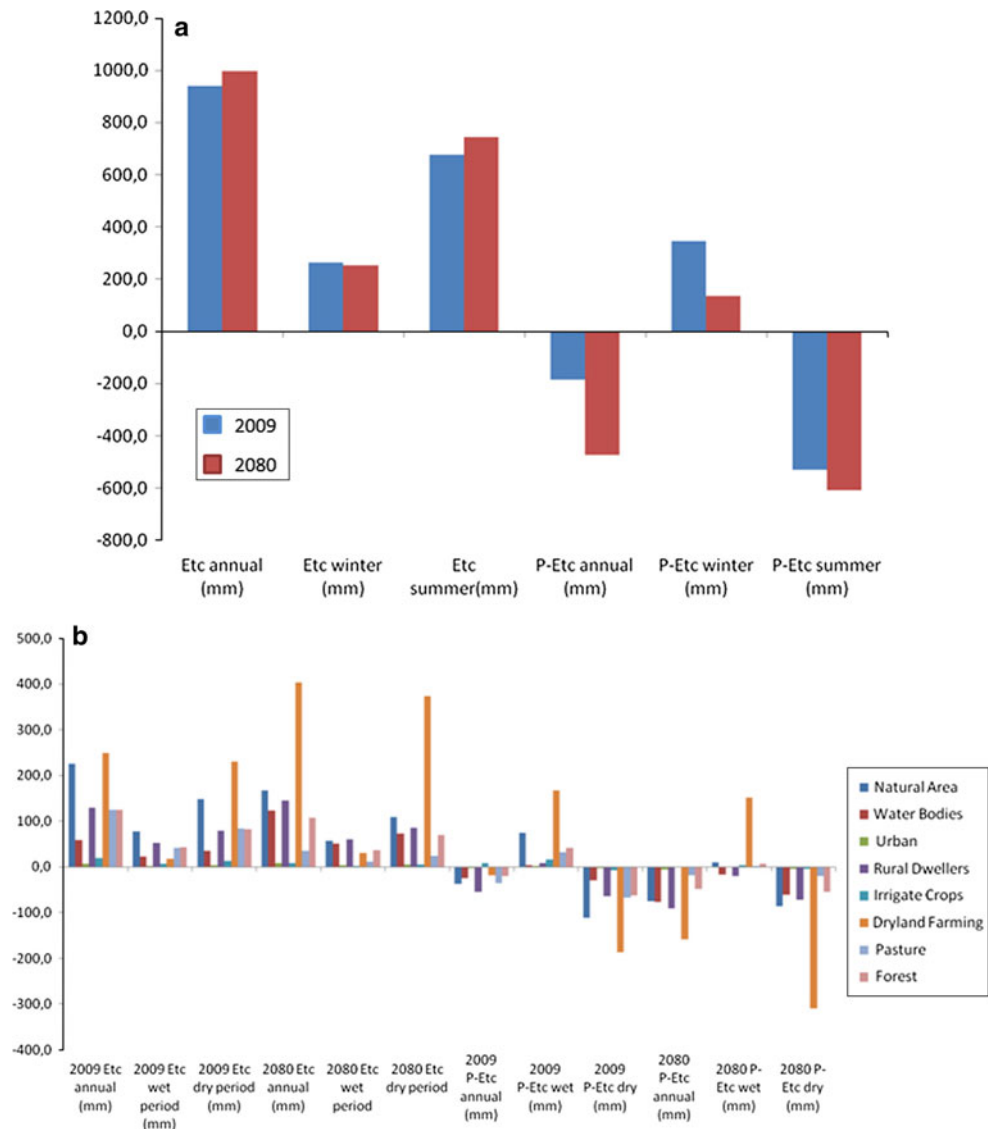
$z_0 = 10$  m and  $\alpha = 0.39$  (Table 4). For a  $0.5$  m sea level rise and an aquifer thickness of  $10$  m, the  $M$  parameter increases by a factor of  $2.8$ .

## Discussion

The results of the spatial interaction model at 2080 compared to the current situation (2009) show a strong decrease in the areas for land suitability classes 1 and 5, which are those allowing for the largest variety of land uses (see Table 3). The coastal zone is the area where there is the largest change in land suitability due to the invasion of sea water in the lowlands ( $5,000$  hectares will be flooded). In the future, therefore, there is an increase in “specialized classes” such as the 2 and the 6 that allow only for dry-land farming and forestry and a loss of those classes of less specialized land use.

The change in land use at the year 2080 with respect to 2009 (Fig. 2a, b) reflects the trends imposed on the territory by the constraints of the climate change SRES A1b scenario and the consequent sea level rise and reduction in rainfall. Besides the flooding of the coastal zone, the most

**Fig. 7 a** Histogram summarizing the simulation results for  $ET_c$  and hydroclimatic deficit (both expressed in equivalent mm of water per unit area) in the Tahadart basin at annual, dry season, and winter season levels. Simulations are for years 2009 and 2080. **b** Histogram showing the individual contributions to  $ET_c$  and hydroclimatic deficit for the different land uses in the Tahadart basin in the years 2009 and 2080



relevant changes in land use from 2009 to the 2080 include the reduction of pastures (from 13,000 hectares in 2009 to 3,000 hectares in 2080) and irrigated crops (from 5,000 hectares in 2009 to 2,000 hectares in 2080) with respect to present time. As a consequence of dryer future conditions there is a strong increase in dry-land farming (from 34,000 hectares in 2009 to 52,000 hectares in 2080). The populations of the Tahadart basin are currently decreasing as many inhabitants have moved to the nearby city of Tangiers where employment is more likely to provide higher income than in the rural area. This trend that has been considered in the spatial interaction model results in diminished attractiveness for the Tahadart as a place where people could live and practice forestry or specialized agriculture such as irrigation farming. The future economic impact, due to the change in agricultural pattern for the area, consists of a decrease in the labor requirements,

resulting in a change in the employment that can result in a further decrease of the local population, if there no substitute labor opportunity in the region for the excess population. Eventually, this employment opportunity could be provided by tourism. The tourism in Moroccan localities such as Agadir and Marrakech has developed fast in the past decade; the Tangiers-Asilah (Tahadart) area has not yet seen the same development but there are signs showing that the area is visited more and more by tourists especially for short stays. Tourism with the associated new developments, hotels, resorts, golf clubs, etc. impacts on local freshwater resources and this in a scenario of climate variability and change may cause problems in the future especially where the climate is semi-arid (He and Hogue 2012).

As expected by the A1b scenario climate models, the increase in temperature at the year 2080 causes an increase



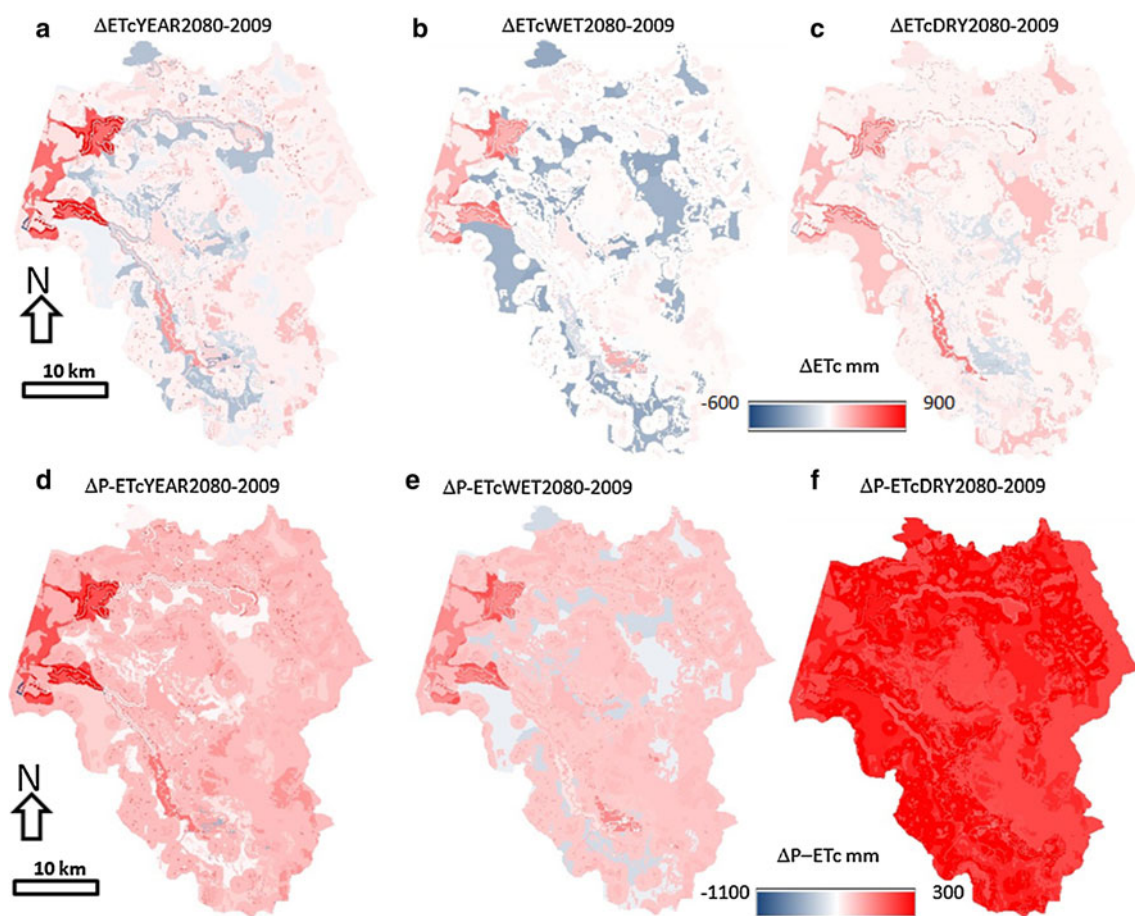


**Fig. 8** Maps of change in  $ET_c$  and hydroclimatic deficit between the years 2009 and 2080 for the Tahadart basin expressed in mm of water per unit area: **a** annual change in  $ET_c$ , **b** “wet” period change in  $ET_c$ ,

**c** “dry” period change in  $ET_c$ , **d** annual change in hydroclimatic deficit, **e** “wet” period change in hydroclimatic deficit, **f** “dry” period change in hydroclimatic deficit

**Table 4** Relative  $M$  values for different, aquifer thickness, sea level rise scenarios, and change in aquifer recharge

$\Delta z$	$\alpha = 1$				$\alpha = 0.39$			
	0	0.5	1	1.5	0	0.5	1	1.5
$M_{cc}$								
$Z_o = 10$	$M$	1.1 $M$	1.2 $M$	1.3 $M$	2.6 $M$	2.8 $M$	3.1 $M$	3.4 $M$
$Z_o = 20$	$M$	1.05 $M$	1.1 $M$	1.2 $M$	2.6 $M$	2.7 $M$	2.8 $M$	3 $M$
$Z_o = 30$	$M$	1.03 $M$	1.07 $M$	1.1 $M$	2.6 $M$	2.64 $M$	2.7 $M$	2.8 $M$

in evaporation and in  $ET_c$  (Fig. 6a, b, 7a) that is more pronounced in the summer (160 mm) with respect to the winter (40 mm). Open water body evaporation is higher than crop or vegetation evapotranspiration, so that an increase in surface water bodies contributes to water salinization and a stronger hydrologic deficit (Mollema et al. 2012).

The increase in evaporation and  $ET_c$  (Table 5) coupled with a decrease in rainfall (from 756 mm in 2009 to 524 mm in 2080) at the year 2080 (A1b scenario) results in a strong increase of the annual hydroclimatic deficit (from

–200 to –500 mm) in the Tahadart basin and a decrease in the winter surplus (from 380 to 160 mm). The decrease in winter surplus has a negative effect on replenishing the reservoirs with water, aquifer recharge and, in the coastal zone (Fig. 6c, d), it promotes salinization of the ground water (Werner et al. 2012). The coastal zone, the water reservoirs, and the urban areas will be the areas mostly stressed by the increase in water budget deficit (Fig. 6c, d). It seems that the water stress will be felt not only in the Tahadart basin during the ‘dry’ period, but also during what today is considered the ‘wet’ period. The changes in



**Table 5** Summary Table for present day and A1b scenario (2080) hydroclimatic parameters

	Landuse	Rainfall	ET <sub>c</sub> /Evap	Deficit/Surplus	Rainfall A1b	ET <sub>c</sub> A1b	Deficit/surplus A1b
Annual	Dry-land farming	755.62	815.9	−60.28	524	860.7745	−336.7745
Winter	Dry-land farming	610.09	60.80	549.29	389	64.144	324.856
Summer	Dry-land farming	145.53	755.10	−609.57	135	796.6305	−661.6305
Annual	Horticulture	755.62	516	239.62	524	544.38	−20.38
Winter	Horticulture	610.09	170	440.09	389	179.35	209.65
Summer	Horticulture	145.53	346	−200.47	135	365.03	−230.03
Annual	Wetlands	755.62	915	−159.38	524	965.325	−441.325
Winter	Wetlands	610.09	339	271.09	389	357.645	31.355
Summer	Wetlands	145.53	576	−430.47	135	607.68	−472.68
Annual	Pine forest	755.62	902	−146.38	524	951.61	−427.61
Winter	Pine forest	610.09	311	299.09	389	328.105	60.895
Summer	Pine forest	145.53	591	−445.47	135	623.505	−488.505
Annual	Open water	755.62	1,309.24	−553.618	524	1,409	−885
Winter	Open water	610.09	520.00	90.086	389	582	−193
Summer	Open water	145.53	789.23	−643.704	135	827	−692

precipitation patterns are felt mostly in winter. The summers currently are already dry and that will not change much in the future. The future winters, however, will be drier than the current ones causing the annual deficits to increase.

An analysis of a possible increase in extreme weather events as predicted to be some of the effects of climate change (IPCC 2007) cannot be easily inferred from the climate model data for the future. It is, however, possible to infer something about the coupled effect of climate and land use change on the effect of storm events and eventual flash floods in the topographically lower areas of the Tahadart basin. By applying the runoff coefficients at the land use scenario of 2080, we have computed that the instantaneous runoff intensity per unit depth of rainfall (1 mm/h) increases of almost 10 %. This increase in runoff intensity may result in an increased soil erosion and in a larger chance of having flooding events in the future.

The evaluation of the vulnerability to salt-water intrusion in the coastal zone of the Tahadart basin was possible only on a relative basis with respect to the current conditions. This was caused by a lack of important data, such as the hydraulic conductivity and the thickness of the aquifer, that are required to quantify parameters such as the depth of the salt water/freshwater interface or the inland extent of the sea water toe (Werner and Simmons 2009; Werner et al. 2012). The analysis of the  $M_{cc}$  indicator for a series of plausible scenarios in the Tahadart coastal zone was nevertheless interesting to pursue. The values of  $M_{cc}$  reported in Table 4 show that the thinner coastal unconfined aquifers are the most vulnerable to salt water intrusion. The sea level rise, if we do not consider the invasion of the lowlands, contributes only from 5 to 30 % in increasing the  $M_{cc}$  value, whereas the decrease of net recharge in 2080 to

39 % of what it was in 2009 has a very strong effect on the  $M_{cc}$  indicator by causing its increase up to 340 % in the worst case scenario. It appears, therefore, that the decrease in winter deficit surplus has the strongest effect on salinization of the coastal ground water.

The methodology presented may help local managers to take decisions based on quantitative data and test multiple possible future scenarios (land cover and climate) in a way to develop rules and policies for better water resources management. One of its major strengths is that it can be easily adapted to the local water management rules, climate conditions, agriculture practices, economic situations, and other kind of watershed's budgets such as those for carbon (Cibien 2011) and nitrogen.

The mitigation measures for the future should be directed to protect against water shortages. This may be done by increasing storage efforts, gathering the excess rain that falls in the winter and during extreme events, to use it later in the dry periods. Where exactly to store this water is a key question, because surface water evaporation will increase and open water reservoirs will lose quickly the stored water. A possible alternative is managed aquifer recharge (MAR) in a way to store surplus water in the aquifers and has the double advantage of creating an extra storage for freshwater and contrasting sea-water intrusion in the coastal zone (Gale 2005).

## Conclusion

The novel workflow methodology adopted in this study is aimed to integrate different kinds of knowledge and data such as socio-economic analysis, land use characterization,

geomorphologic analysis, climate data, hydrological models, spatial interaction models, and future climate models under the IPCC SRES scenario A1b. The integration has been aided by means of GIS software and spreadsheet-based elaboration tools such as WATER\_DST, a visualization and computation tool that displays and quantifies immediately on screen the effects of land use change on the hydrological budget of a watershed.

The application of this methodology to the Tahadart basin has allowed to quantify the effect of land use and climate change under SRES scenario A1b at the end of this century on freshwater resources. The results show an increase of the deficit in the annual water budget and a decrease of the winter surplus by more than half the present value. This increase in water deficit will drive a change in land use and will cause an increase in the areas that are suitable for dry-land farming and a strong decrease in areas adapt for pasture, horticulture, and forestry. At the same time, the decrease in winter water surplus causes a decrease in the net recharge of the coastal unconfined aquifer that results in a possible increase of ground water salinization. Sea level rise will cause the flooding of the current lowlands adjacent to the Tahadart estuary. As a result of climate change and the socio-economic development, which indicates a strong increase of the tourism industry in the Tahadart basin, the freshwater resources will be under more pressure in the future and their management has to become a priority for the local administrators.

**Acknowledgments** This work has been carried out in the framework of the WATERKNOW project funded by the European CIRCLEMED (2011) initiative for the development of knowledge to counteract the effects of climate change on the water cycle in the Mediterranean. We thank also Andrea Minchio, Mario Laghi, and Elizabeth General Diaz for helping in data elaboration. Reviews of Tibor Stigter, Nicolas Faysse, and two anonymous have greatly improved the manuscript.

## References

- Batelaan O, De Smedt F (2007) GIS-based recharge estimation by coupling surface–subsurface water balances. *J Hydrol* 337:337–355
- Blaschke T (2010) Object based image analysis for remote sensing. *ISPRS* 65:2–16
- Carneiro JF, Boughriba M, Correia A, Zarhloule Y, Rimi A, El Houadi B (2010) Evaluation of climate change effects in a coastal aquifer in Morocco using a density-dependent numerical model. *Environ Earth Sci* 61:241–252
- Cibien M (2011) Riforestazione e gestione dell'uso del suolo come metodo di cattura della CO<sub>2</sub> contro i cambiamenti climatici nella zona costiera di Ravenna (Reforestation and soil management as a method to store CO<sub>2</sub> and mitigate climate change in the coastal zone of Ravenna, Italy). MSc Dissertation, University of Bologna. <http://amslaurea.cib.unibo.it/2501>
- CORINE LAND COVER (2011) Final report <http://www.eea.europa.eu/publications/COR0>. Accessed 14 Jun 2011
- CROPWAT (2011) Software description [http://www.fao.org/nr/water/infores\\_databases\\_cropwat.html](http://www.fao.org/nr/water/infores_databases_cropwat.html). Accessed 14 Jun 2011
- Custodio E (2010) Coastal aquifers of Europe: an overview. *Hydrogeol J* 18:269–280
- Dentinho TP, Silveira P (2010) Spatial Interaction Model with Land Use to Analyze the Impact of Designed Accessibilities. An Application to Corvo Island from XVI, XIX and XX Centuries. *Comput Environ Urban Sys* 34:91–103
- European Union Commission (2009) Integrated Coastal Zone Management Protocol. Off J Eur Union L34:19–28
- European Union Commission (2010) EU Focus on the coastal zone. EEA publications, Bruxelles
- Fernandes PG, Carreira PM, Bahir M (2010) Mass balance simulation and principal components analysis applied to ground water resources: essaouira basin (Morocco). *Environ Earth Sci* 59:1475–1484
- Fetter CW (2001) Applied hydrogeology. Prentice hall, New Jersey
- Fox HR, Moore HM, Newell Price JP, El Kasri M (1997) Soil erosion and reservoir sedimentation in the High Atlas Mountains, southern Morocco. In: Proceedings of the Symposium on Human Impact on Erosion and Sedimentation, Rabat, Morocco, IAHS, vol 24, pp 233–240
- Gale I (2005) Strategies for managed aquifer recharge (MAR) in semi-arid areas. UNESCO IHP, Paris
- Gao J, Skillkorn D (1998) Capability of SPOT XS data in producing detailed land cover maps at the urban-rural periphery. *Int J Remote Sens* 19:2877–2899
- Giupponi C, Mordechai S (2003) Climate Change in the Mediterranean. Edward Elgar Publishing, Northampton
- Giupponi C (2007) Decision support systems for implementing the European Water Framework Directive: the MULINO approach. *Environ Model Software* 22:248–258
- He MX, Hogue TS (2012) Integrating hydrologic modeling and land use projections for evaluation of hydrologic response and regional water supply impacts in semi-arid environments. *Environ Earth Sci* 65:1671–1685
- Healy RW (2011) Estimating Ground water Recharge. Cambridge University Press, Cambridge
- IPCC (2007) Climate Change 2007, the Fourth IPCC Assessment Report. IPCC publications, Geneva
- Kalbacher T, Delfs JO, Shao HB, Wang WQ, Walther M, Samaniego L, Schneider C, Kumar R, Musolff A, Centler F, Sun F, Hildebrandt A, Liedl R, Borchardt D, Krebs P, Kolditz O (2012) Software coupling for an integrated water resources management. *Environ Earth Sci* 65:1367–1380
- Maidment DR (1992) Handbook of Hydrology. McGraw-Hill, New York
- Mollema PN, Antonellini M, Gabbianelli G, Laghi M, Marconi V, Minchio A (2012) Climate and water budget change of a Mediterranean coastal watershed, Ravenna, Italy. *Environ Earth Sci* 65:257–276
- Mollema PN, Antonellini M (2013) Seasonal variation in natural recharge of coastal aquifers. *Hydrogeol J* (HJ-2012-2390 in press)
- Monteith JL (1973) Principles of Environmental Physics. Edward Arnold, London
- Penman HL (1948) Natural evaporation from open water, bare soil and grass. *Proc R Soc London A* 193:120–146
- PRUDENCE (2011) Final report <http://prudence.dmi.dk>. Accessed 27 Jun 2011
- Revenga C, Murray S, Abramovitz J, Hammond A (1998) Watersheds of the world: ecological value and vulnerability. World Resources Institute, Washington
- Saxton KE (2003) Soil water characteristics Version 6.5.51. A computer program for calculating soil properties. USDA Agricultural Research Service and Department of Biological Systems Engineering, Washington State University

- Schanze J, Trumper J, Burmeister C, Pavlik D, Kruhlov I (2012) A methodology for dealing with regional change in integrated water resources management. *Environ Earth Sci* 65:1405–1414
- Silveira P, Silva V, Dentinho TP (2009) Spatial interaction model with land and water use: An application to Terceira Island. In: *Proceedings 45th ISOCARP Congress*, p 17
- Small C, Nicholls RJ (2003) A global analysis of human settlements in coastal zones. *J Coastal Res* 19:584–599
- Smith M, Allen RG, Monteith JL, Perrier A, Pereira L, Segeren A (1992) Report of the expert consultation on procedures for revision of FAO guidelines for prediction of crop water requirements. UN-FAO, Rome
- Solomon S, Qin D, Manning M, Chen Z, Marquis M, Averyt KB, Tignor M, Miller HL (2007) Contribution of Working Group I to the Fourth Assessment Report of the Intergovernmental Panel on Climate Change. Cambridge University Press, Cambridge
- Trabelsi R, Abid K, Zouari K, Yahyaoui H (2012) Ground water salinization processes in shallow coastal aquifer of Djeffara plain of Medenine, Southeastern Tunisia. *Environ Earth Sci* 66: 641–653
- Vallega A (1999) *Fundamental of coastal zone management*. Kluwer, Dordrecht
- Werner AD, Simmons CT (2009) Impact of sea-level rise on sea water intrusion in coastal aquifers. *Ground Water* 47:197–204
- Werner AD, Ward JD, Morgan LK, Simmons CT, Robinson NI, Teubner MD (2012) Vulnerability indicators of sea water intrusion. *Ground Water* 50:48–58